Electronic Supplementary Information for Theoretical Study on the Anisotropic Photo-Induced Carrier Mobilities in Layered Double Hydroxides-Based Photocatalysts

Zi-Ru Chen,[#a] Yu-Quan Zhu,[#a] Si-Min Xu,[*ab] Yufei Zhao,[a] Qian Peng,[*b] and Hong Yan[*a]

a State Key Laboratory of Chemical Resource Engineering, Beijing University of Chemical Technology, Beijing 100029, P. R. China

b State Key Laboratory of Elemento Organic Chemistry, College of Chemistry, Nankai University, Tianjin 300071, P. R. China

# Zi-Ru Chen and Yu-Quan Zhu contributed equally to this work

Corresponding Authors

Si-MinXu@mail.buct.edu.cn, Si-MinXu@nankai.edu.cn, xsm713@sina.com (S.-M. Xu.),

qpeng@nankai.edu.cn (Q. Peng),

yanhong@mail.buct.edu.cn (H. Yan)

Contents

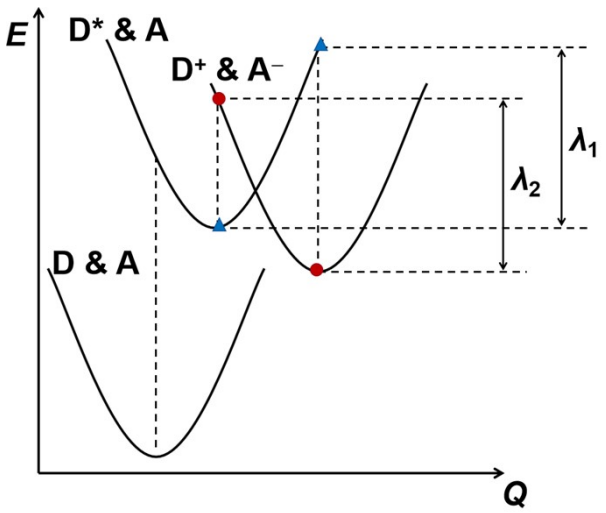

Fig. S1. Schematic illustration of the compositions of internal reorganization energy λ in Marcus theory. The curves represent the potential energy surfaces of D & A (D represents the donor in the ground state, A denotes the acceptor in the ground state), and D^+ & A^- (D^+ represents the donor in the cationic state and A^- represents the acceptor in the anionic state), D* & A (D* represents the donor in the excited state), respectively.

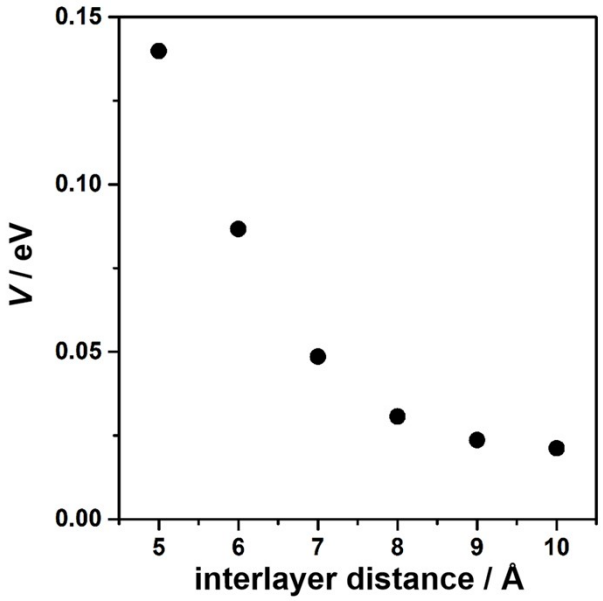

Fig. S2. Relationship between the transfer integral *V* and interlayer distance between two LDHs matrix in $[Mg_2Al(OH)_6(OH_2)_7]\cdot Cl$.

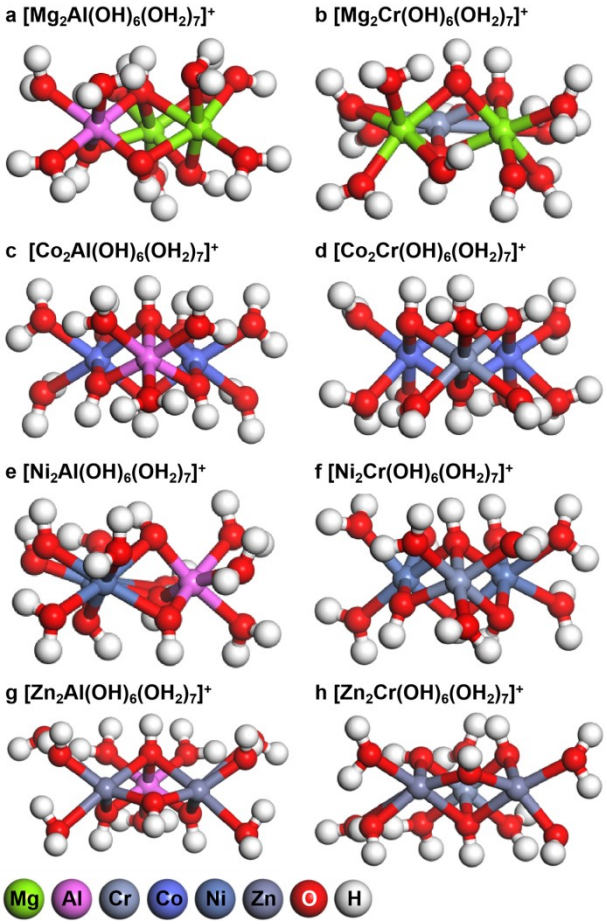

Fig. S3. Optimized geometries of (a) $[Mg_2Al(OH)_6(OH_2)_7]^+$, (b) $[Mg_2Cr(OH)_6(OH_2)_7]^+$, (c) $[Co_2Al(OH)_6(OH_2)_7]^+$, (d) $[Co_2Cr(OH)_6(OH_2)_7]^+$, (e) $[Ni_2Al(OH)_6(OH_2)_7]^+$, (f) $[Ni_2Cr(OH)_6(OH_2)_7]^+$, (g) $[Zn_2Al(OH)_6(OH_2)_7]^+$, and (h) $[Zn_2Cr(OH)_6(OH_2)_7]^+$ cluster models. The color of each element is labeled.

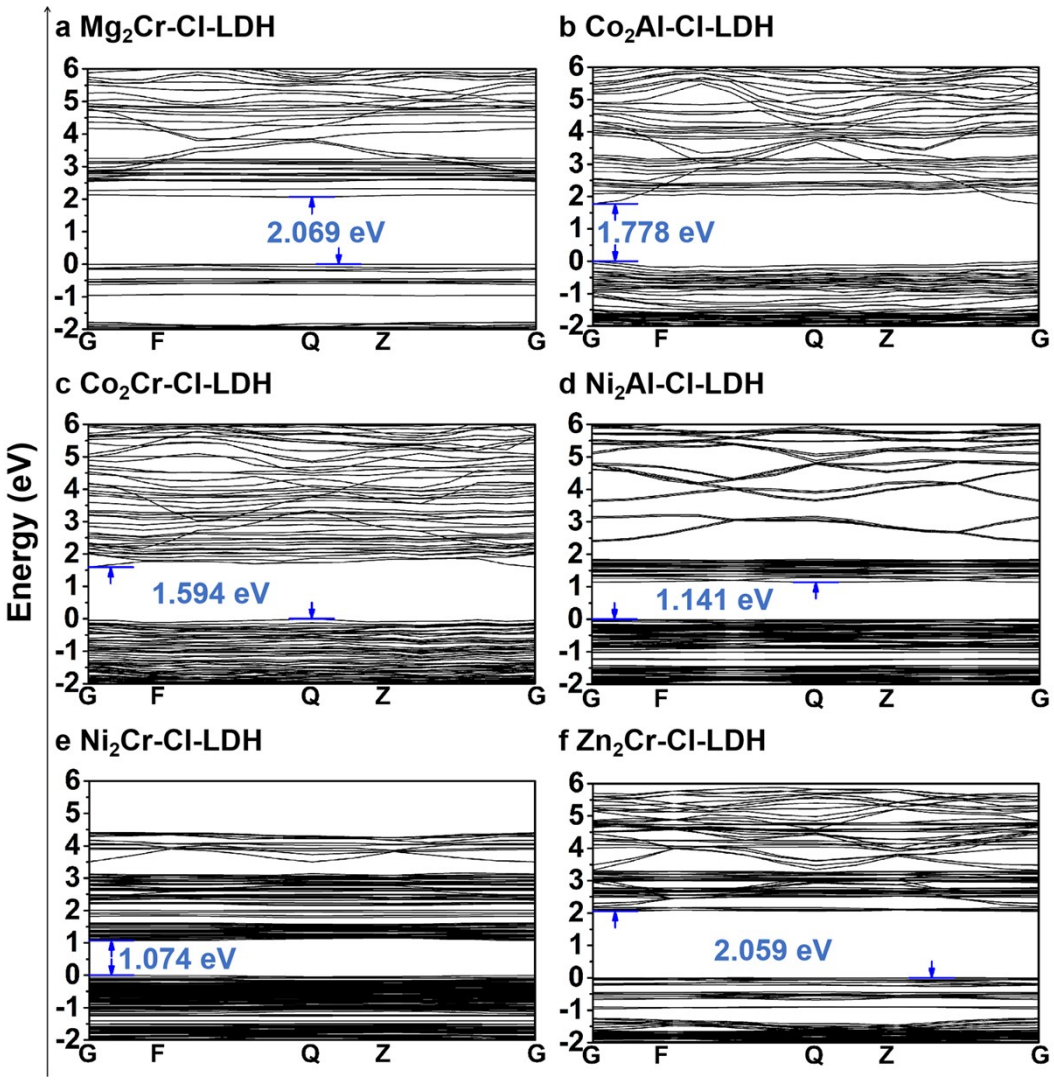

Fig. S4. Band Structures of (a) Mg_2Cr-Cl-LDH, (b) Co_2Al-Cl-LDH, (c) Co_2Cr-Cl-LDH, (d) Ni_2Al-Cl-LDH, (e) Ni_2Cr-Cl-LDH, and (f) Zn_2Cr-Cl-LDH at the level of PBE. The valence band maximums, conduction band minimums, and band gap energies are labeled.

Table S1. Experimental and Calculated (with and without van der Waals Correction) Lattice Parameters for Periodic Models of M_2M'-Cl-LDHs (M = Mg, Co, Ni, and Zn; M' = Al, and Cr)

model	lattice parameter (Å)					
	experimental		calculated			
			without van der Waals correction		with van der Waals correction	
	$a = b$	c	$a = b$	c	$a = b$	c
Mg_2Al-Cl-LDH	3.04[S1]	7.54[S1]	3.08	7.49	3.07	7.38
Mg_2Cr-Cl-LDH	3.01[S2]	7.72[S3]	3.10	7.58	3.11	7.50
Co_2Al-Cl-LDH	3.07[S4]	7.59[S4]	3.07	7.59	3.05	7.52
Co_2Cr-Cl-LDH	3.08[S5]	7.86[S6]	3.08	7.73	3.08	7.70
Ni_2Al-Cl-LDH	3.01[S7]	7.64[S7]	3.03	8.05	3.03	7.78
Ni_2Cr-Cl-LDH	3.08[S8]	7.74[S8]	3.07	8.66	3.07	8.28
Zn_2Al-Cl-LDH	3.08[S9]	7.80[S9]	3.11	7.81	3.10	7.81
Zn_2Cr-Cl-LDH	3.11[S10]	7.71[S10]	3.15	7.73	3.15	7.72

Table S2. Structural Information for the Optimized Geometries of $[Mg_2Al(OH)_6(OH_2)_7]\cdot Cl$, $[Mg_4Al_2(OH)_{12}(OH_2)_{10}]\cdot 2Cl$, and $[Mg_6Al_3(OH)_{18}(OH_2)_{12}]\cdot 3Cl$ Cluster Models

model	distance (Å)		bond length (Å)	
	Mg-Mg	Mg-Al	Mg-O	Al-O
$[Mg_2Al(OH)_6(OH_2)_7]\cdot Cl$	3.073	3.015	2.294	1.920
$[Mg_4Al_2(OH)_{12}(OH_2)_{10}]\cdot 2Cl$	2.981	3.031	2.261	1.932
$[Mg_6Al_3(OH)_{18}(OH_2)_{12}]\cdot 3Cl$	3.152	3.092	2.157	1.932
model	bond angle (°)			dihedral angle (º)
	Mg-O-Mg	O-Mg-O	O-Al-O	O-Al-O-Mg
$[Mg_2Al(OH)_6(OH_2)_7]\cdot Cl$	97.122	89.105	87.092	176.715
$[Mg_4Al_2(OH)_{12}(OH_2)_{10}]\cdot 2Cl$	92.938	76.663	87.286	173.455
$[Mg_6Al_3(OH)_{18}(OH_2)_{12}]\cdot 3Cl$	95.401	81.328	86.255	174.054

Table S3. Structural Information for the Optimized Geometries of $[M_2M'(OH)_6(OH_2)_7]\cdot Cl$ Cluster Models (M = Mg, Co, Ni, and Zn; M' = Al, and Cr)

model	distance (Å)		bond length (Å)	
	M-M	M-M'	M-O	M'-O
$[Mg_2Al(OH)_6(OH_2)_7]^+$	3.035	3.003	2.295	1.921
$[Mg_2Cr(OH)_6(OH_2)_7]^+$	3.030	3.092	2.278	1.996
$[Co_2Al(OH)_6(OH_2)_7]^+$	3.207	2.951	2.218	1.920
$[Co_2Cr(OH)_6(OH_2)_7]^+$	3.156	3.140	2.300	1.988
$[Ni_2Al(OH)_6(OH_2)_7]^+$	2.857	3.255	2.410	1.936
$[Ni_2Cr(OH)_6(OH_2)_7]^+$	3.027	3.022	2.255	1.996
$[Zn_2Al(OH)_6(OH_2)_7]^+$	3.126	3.051	2.325	1.921
$[Zn_2Cr(OH)_6(OH_2)_7]^+$	3.081	3.098	2.283	1.994
model		angle (º)		dihedral angle (º)
	M-O-M	O-M-O	O-M'-O	O-M'-O-M
$[Mg_2Al(OH)_6(OH_2)_7]^+$	95.227	85.852	87.265	175.627
$[Mg_2Cr(OH)_6(OH_2)_7]^+$	95.741	75.209	85.209	176.489
$[Co_2Al(OH)_6(OH_2)_7]^+$	99.012	83.343	88.172	172.560
$[Co_2Cr(OH)_6(OH_2)_7]^+$	99.116	80.819	86.238	176.947
$[Ni_2Al(OH)_6(OH_2)_7]^+$	72.844	67.444	90.543	147.219
$[Ni_2Cr(OH)_6(OH_2)_7]^+$	97.661	82.916	86.724	170.754
$[Zn_2Al(OH)_6(OH_2)_7]^+$	96.993	74.797	86.561	175.534
$[Zn_2Cr(OH)_6(OH_2)_7]^+$	97.460	76.706	87.480	176.029

Table S4. Band Gap Energies (E_g), Work Functions (W), Valence Band Maximum (E_{VBM}), and Conduction Band Minimum (E_{CBM}) for M_2M'-Cl-LDHs (M = Mg, Co, Ni, and Zn; M' = Al, and Cr) under Lattice Dilation and Compression in x and y Directions

model	direction	$\Delta l / l_0$	E_g (eV)	W (eV)	E_{VBM} / eV	E_{CBM} / eV
Mg_2Al-Cl-LDH	x	−1%	4.357	4.847	−5.305	−0.973
		−0.5%	4.344	4.853	−5.248	−0.904
		0%	4.333	4.860	−5.100	−0.812
		0.5%	4.332	4.500	−5.020	−0.738
		1%	4.319	4.871	−4.970	−0.651
	y	−1%	4.353	4.662	−5.255	−0.641
		−0.5%	4.338	4.610	−5.238	−0.686
		0%	4.311	4.699	−5.207	−0.697
		0.5%	4.293	4.661	−5.389	−0.715
		1%	4.274	4.634	−5.371	−0.744
Mg_2Cr-Cl-LDH	x	−1%	2.867	4.237	–6.383	–3.504
		−0.5%	2.836	4.365	–6.351	–3.547
		0%	2.824	4.259	–6.270	–3.581
		0.5%	2.768	4.232	–6.246	–3.618
		1%	2.742	4.229	–6.200	–3.647
	y	−1%	2.819	4.230	–6.285	–3.521
		−0.5%	2.806	4.282	–6.260	–3.542
		0%	2.803	4.259	–6.241	–3.549
		0.5%	2.791	4.245	–6.239	–3.558
		1%	2.775	4.230	–6.218	–3.579
Co_2Al-Cl-LDH	x	−1%	2.626	5.547	–6.860	–4.234
		−0.5%	2.581	5.563	–6.854	–4.272
		0%	2.651	5.580	–6.906	–4.254
		0.5%	2.584	5.608	–6.900	–4.316
		1%	2.650	5.623	–6.948	–4.298
	y	−1%	2.615	5.449	–6.757	–4.141
		−0.5%	2.632	5.494	–6.810	–4.178
		0%	2.651	5.580	–6.906	–4.254
		0.5%	2.644	5.634	–6.956	–4.312
		1%	2.651	5.690	–7.015	–4.365
Co_2Cr-Cl-LDH	x	−1%	2.239	4.369	–7.937	–5.581
		−0.5%	2.254	4.312	–7.969	–5.549
		0%	2.269	4.416	–7.989	–5.502
		0.5%	2.279	4.297	–8.002	–5.485
		1%	2.301	4.352	–8.051	–5.458

		–1%	2.237	4.619	–7.938	–5.501
		–0.5%	2.242	4.687	–7.954	–5.512
	y	0%	2.251	4.628	–7.986	–5.530
		0.5%	2.297	4.658	–8.008	–5.544
		1%	2.292	4.680	–8.026	–5.566
		–1%	2.565	4.671	–5.953	–3.389
		–0.5%	2.567	4.647	–5.937	–3.364
	x	0%	2.588	4.629	–5.930	–3.343
		0.5%	2.594	4.640	–5.923	–3.335
		1%	2.597	4.602	–5.901	–3.303
Ni_2Al-Cl-LDH		–1%	2.294	4.672	–5.819	–3.525
		–0.5%	2.322	4.609	–5.806	–3.468
	y	0%	2.338	4.637	–5.800	–3.448
		0.5%	2.355	4.622	–5.770	–3.404
		1%	2.371	4.562	–5.748	–3.377
		–1%	2.079	4.843	–5.883	–3.803
		–0.5%	2.094	4.793	–5.840	–3.746
	x	0%	2.163	4.720	–5.802	–3.638
		0.5%	2.146	4.696	–5.769	–3.623
		1%	2.092	4.669	–5.715	–3.623
Ni_2Cr-Cl-LDH		–1%	2.115	4.550	–5.608	–3.492
		–0.5%	2.059	4.633	–5.663	–3.603
	y	0%	2.163	4.720	–5.802	–3.638
		0.5%	2.085	4.774	–5.816	–3.732
		1%	2.110	4.824	–5.879	–3.769
		–1%	3.401	4.854	−5.961	−2.453
		–0.5%	3.405	4.848	−5.955	−2.445
	x	0%	3.417	4.852	−5.951	−2.444
		0.5%	3.408	4.838	−5.942	−2.434
		1%	3.411	4.829	−5.935	−2.424
Zn_2Al-Cl-LDH		–1%	3.382	4.848	−5.942	−2.458
		–0.5%	3.384	4.850	−5.939	−2.457
	y	0%	3.389	4.841	−5.936	−2.446
		0.5%	3.391	4.835	−5.930	−2.440
		1%	3.388	4.833	−5.927	−2.439
		–1%	2.466	5.031	–6.264	–3.798
		–0.5%	2.459	5.055	–6.285	–3.825
	x	0%	2.478	5.065	–6.304	–3.826
		0.5%	2.424	5.074	–6.286	–3.862
Zn_2Cr-Cl-LDH		1%	2.409	5.077	–6.282	–3.872
		–1%	2.495	4.868	–6.116	–3.620
		–0.5%	2.497	4.957	–6.205	–3.709
	y	0%	2.478	5.065	–6.304	–3.826
		0.5%	2.436	5.152	–6.370	–3.934

	1%	2.390	5.215	–6.410	–4.020

References

(S1) L. Sun and W. Tang, Preparation of Layered Double Hydroxides Nanomaterials *via* the Anionic Surfactant, *Appl. Mech. Mater.*, 2012, **155–156**, 907–911.

(S2) K. Maeda and K. Domen, Photocatalytic Water Splitting: Recent Progress and Future Challenges, *J. Phys. Chem. Lett.*, 2010, **1**, 2655–2661.

(S3) I. M. Ahmed, Mg-Cr Layered Double Hydroxide (LDH) Intercalated with Sodium Dodecyl Sulfate as Sorbent for Alizarine Red-S in Aqueous Solutions, *Arab J. Nucl. Sci. Appl.*, 2021, **54**, 50–62.

(S4) B. Grégoire, C. Ruby and C. Carteret, Structural Cohesion of M^{II}-M^{III} Layered Double Hydroxides Crystals: Electrostatic Forces and Cationic Polarizing Power, *Cryst. Growth Des.*, 2012, **12**, 4324–4333.

(S5) H. Pourradi, K. Ghani and M. Mahdavi, Fully Ambient Air Processed Perovskite Solar Cell Based on $Co(Co,Cr)_2O_4/TiO_2$ P-N Heterojunction Array in Photoanode, *J. Phys. Chem. C*, 2019, **123**, 4044–4055.

(S6) F. Cavani, F. Trifiro and A. Vaccari, Hydrotalcite-Type Anionic Clays: Preparation, Properties and Applications, *Catal. Today*, 1991, **11**, 173–301.

(S7) M. E. Pérez-Bernal, R. J. Ruano-Casero, F. Benito and V. Rives, Nickel-Aluminum Layered Double Hydroxides Prepared *via* Inverse Micelles Formation, *J. Solid State Chem.*, 2009, **182**, 1593–1601.

(S8) O. Clause, M. Gazzano, F. Trifiro', A. Vaccari and L. Zatorski, Preparation and Thermal Reactivity of Nickel/Chromium and Nickel/Aluminium Hydrotalcite-Type Precursors, *Appl. Catal.*, 1991, **73**, 217–236.

(S9) S. Vial, C. Forano, D. Shan, C. Mousty, H. Barhoumi, C. Martelet and N. Jaffrezic, Nanohybrid-Layered Double Hydroxides/Urease Materials: Synthesis and Application to Urea Biosensors, *Mater. Sci. Eng. C*, 2006, **26**, 387–393.

(S10) L. E. Mersly, E. Mountassir, E. M. Moujahid, C. Forano, M. E. Haddad, S. Briche, A. A. Tahiri and S. Rafqah, ZnCr-LDHs with Dual Adsorption and Photocatalysis Capability for the Removal of Acid Orange 7 Dye in Aqueous Solution, *J. Sci-Adv. Mater. Dev.*, 2021, **6**, 118–126.